
THE RADIAL POINT INTERPOLATION MIXED COLLOCATION (RPIMC) METHOD FOR THE SOLUTION OF TRANSIENT DIFFUSION PROBLEMS

A PREPRINT

Konstantinos A. Mountris*

Aragón Institute of Engineering Research, IIS Aragón
University of Zaragoza
Spain, Zaragoza, ZGZ 50018
kmountris@unizar.es

Esther Pueyo

Aragón Institute of Engineering Research, IIS Aragón,
CIBER-BBN
University of Zaragoza
Spain, Zaragoza, ZGZ 50018
epueyo@unizar.es

May 26, 2022

ABSTRACT

The Radial Point Interpolation Mixed Collocation (RPIMC) method is proposed in this paper for transient analysis of diffusion problems. RPIMC is an efficient purely meshless method where the solution of the field variable is obtained through collocation. The field function and its gradient are both interpolated (mixed collocation approach) leading to reduced C -continuity requirement compared to strong-form collocation schemes. The method's accuracy is evaluated in heat conduction benchmark problems. The RPIMC convergence is compared against the Meshless Local Petrov-Galerkin Mixed Collocation (MLPG-MC) method and the Finite Element Method (FEM). Due to the delta Kronecker property of RPIMC, improved accuracy can be achieved as compared to MLPG-MC. RPIMC is proven to be a promising meshless alternative to FEM for transient diffusion problems.

Keywords RPIMC · meshless · radial point interpolation · mixed collocation · diffusion · heat conduction

*[mail] kmountris@unizar.es [url] <https://www.mountris.org>

1 Introduction

The diffusion equation describes many physical phenomena where motion is driven by the gradient of the field variable. Time-dependent problems like heat and mass transport [1], unsteady viscous fluid flow [2] and magneto-hydrodynamics flow [3] can be solved by the transient diffusion equation. Also, the diffusion equation appears in the description of coupled phenomena, such as the transport of chemical or biological reactions by diffusive propagation in a medium (reaction-diffusion phenomena) [4]. Mathematically, reaction-diffusion problems are described by a coupled set of ordinary differential equations (ODEs) that describes the reactive term and a partial differential equation (PDE) that describes the diffusive term. Usually, a much smaller time scale is required for the reactive term than for the diffusive term and operator splitting techniques are used to decouple the problem and compute a numerical solution efficiently [5, 6]. Among the various available methods to solve the PDE of the diffusive term, of great interest are the Meshless Methods (MMs).

MMs, in contrast to mesh-based methods, do not require connectivity information for the construction of basis functions. Therefore, domains with irregular geometry, nonlinearity and discontinuity can be treated efficiently. The use of MMs to solve both the steady and transient diffusion equation has been extensively reported. Steady-state heat conduction in isotropic and functionally graded materials has been solved successfully by the Meshless Point Collocation (MPC) method [7]. In [8], an explicit collocation method with local Radial Basis Functions (RBFs) has been successfully applied to solve the transient diffusion equation in two-dimensional (2D) domains with both regular and irregular nodal discretization. The collocation methods demonstrate high efficiency due to the compact support and the small bandwidth in linear algebraic systems. However, accuracy is deteriorated near the Neumann boundaries due to the requirement for the approximation of spatial derivatives, which is significantly less accurate than the approximation of the field variable [9]. On the other hand, in the Element Free Galerkin (EFG) meshless method [10], which is based on the Galerkin weak formulation, the Neumann boundary conditions (BCs) are satisfied naturally, similarly to the Finite Element Method (FEM). In EFG, the FEM basis functions are replaced with the Moving Least Squares (MLS) basis functions and, hence, no mesh is required for the construction of the trial and test functions. However, the notion of a background mesh is introduced for the generation of quadrature points and the evaluation of the weak form's spatial integrals. Application of EFG for the solution of heat transfer problems has been rigorously explored [11, 12, 13]. Moreover, the improved MLS (IMLS) approximants have been proposed to improve the handling of Dirichlet BC and the efficiency of EFG for three-dimensional (3D) heat conduction problems [14]. Maximum entropy approximants that possess the weak-Kronecker delta property for direct imposition of the Dirichlet BC have also been proposed in the framework of EFG [15, 16, 17].

To alleviate the background mesh requirement of EFG, MMs based on the local Petrov-Galerkin weak form have been proposed, based on the pioneering work on the Meshless Local Petrov-Galerkin (MLPG) method [18, 19, 20]. In MLPG, quadrature points are generated in individual local quadrature domains centered at each field node and the trial and test functions can be selected from different spaces. The flexibility in the selection of the test functions offers the possibility to construct different variations of the MLPG method [21]. In the common MLPG, a spline function (usually quartic) is used as the test function and the MLS as the trial function. By selecting the Heaviside function as the test function, the local weak form is simplified and integrals are evaluated only at the boundaries, leading to a significant increase in time efficiency [22]. By choosing the Dirac function as the test function and interpolating both the field function and its gradient, the MLPG Mixed Collocation (MLPG-MC) method is derived [23]. MLPG-MC has minimum computational cost since no integration is performed. Compared to standard collocation methods, MLPG-MC demonstrates reduced deterioration at the Neumann boundaries, as the order of the spatial derivatives is reduced through the interpolation of the field function's gradient. The MLPG-MC method has been successfully applied to solve inverse Cauchy problems for steady-state heat transfer [24]. Variations of the MLPG method using different trial functions have been investigated extensively [25, 26]. Since MLS basis functions do not possess the delta Dirac property, special treatment to impose the Dirichlet BC is required. To address this issue, the Local Radial Point Interpolation (LRPIM) [27] method was proposed, in which the MLS basis functions are replaced with Radial Point Interpolation (RPI). The RPI basis functions possess the Kronecker delta property and Dirichlet BC imposition is straightforward, as in FEM and maximum entropy approximants. The LRPIM has been used to successfully solve problems in free vibration analysis [28], incompressible flow [27], material non-linearity [29] and transient heat conduction [30], among others. Finally, a hybrid meshfree weak-strong form method has been proposed where LRPIM is used only for nodes near and on the Neumann boundary while for the rest of nodes the strong form collocation method is used [31]. This method combines the time efficiency of collocation methods and the accurate treatment of Neumann BC of LRPIM. However, to our knowledge, up to now RPI has not been evaluated in the mixed collocation variant.

The purpose of the present study is to investigate the performance of the mixed collocation method using the RPI basis functions for the solution of transient diffusion problems. A motivation of this work is subsequent application of the

evaluated method to solve the monodomain reaction-diffusion equation for action potential propagation in the human heart [32]. The standard approach to solve the monodomain model involves the operator splitting method. It is for that reason that in this study the solution to pure transient diffusion problems is considered. Without loss of generality, the method is evaluated in 2D and 3D benchmark problems of transient heat conduction. The structure of the paper is the following. In section 2, the theory of the RPI basis functions is reviewed. In section 3, the mathematical formulation and implementation details of the Radial Point Interpolation Mixed Collocation (RPIMC) method are presented. In section 4, the RPIMC method is evaluated in 2D and 3D heat conduction benchmark problems. Finally, in section 5 some concluding remarks are provided.

2 Radial point interpolation review

In RPI, RBFs augmented with polynomials are used to approximate the field function. In contrast to MLS, RPI possesses the Kronecker delta property, therefore essential boundary conditions are imposed directly. For any field function $u(\mathbf{x})$, defined in the domain $\Omega \subset \mathbb{R}^d$, the RPI approximation $u^h(\mathbf{x}_I)$ at a point of interest $\mathbf{x}_I \in \mathbb{R}^d$ is given by:

$$u^h(\mathbf{x}_I) = \sum_{i=1}^n r_i(\mathbf{x}_I) a_i(\mathbf{x}_I) + \sum_{j=1}^m p_j(\mathbf{x}_I) b_j(\mathbf{x}_I) = \mathbf{r}^T(\mathbf{x}_I) \mathbf{a}(\mathbf{x}_I) + \mathbf{p}^T(\mathbf{x}_I) \mathbf{b}(\mathbf{x}_I) \quad (1)$$

where $r_i(\mathbf{x}_I)$ are the RBFs and $p_j(\mathbf{x}_I)$ are the polynomial basis functions, $a_i(\mathbf{x}_I)$ and $b_j(\mathbf{x}_I)$ denote the corresponding coefficients, n is the number of neighbor nodes in the local support domain of \mathbf{x}_I , and m is the number of polynomial terms. In Equation (1), different forms of RBFs can be used to represent $r_i(\mathbf{x}_I)$. In this study, we use the Multi-Quadric RBFs (MQ-RBFs) due to their satisfactory performance reported in previous studies [31, 26]. In 2D, the MQ-RBFs are given by:

$$r_i(\mathbf{x}_I) = (d_{Ii}^2 + r_c^2)^q = [(x_I - x_i)^2 + (y_I - y_i)^2 + r_c^2]^q \quad (2)$$

where r_c and q are positive-valued shape parameters of the MQ-RBF and d_{Ii} is the Euclidean norm between the point of interest $\mathbf{x}_I = (x_I, y_I)$ and the i^{th} neighbor node $\mathbf{x}_i = (x_i, y_i)$. Analogous MQ-RBFs are defined in 3D. Rectangular or cuboid local support domains for 2D and 3D problems, respectively, are constructed in this study. Following the notation in [31], the shape parameter r_c is given by:

$$r_c = \alpha_c d_c \quad (3)$$

where α_c is a dimensionless constant and d_c denotes the average nodal spacing in the proximity of the point of interest \mathbf{x} . The effect of the choice of α_c and q on the approximation accuracy has been investigated in [33, 27]. In this study, parameter values $\alpha_c = 1.5$ and $q = 1.03$ are used in all the benchmark problems of section 4.

The k^{th} order polynomial basis function $p(\mathbf{x})$ in Equation (1) is given by:

$$\mathbf{p}(\mathbf{x}) = \mathbf{p}(x, y) = \{1, x, y, xy, x^2, y^2, \dots, x^k, y^k\}^T. \quad (4)$$

In this work, we use the linear polynomial basis functions ($k = 1$). The coefficients $a_i(\mathbf{x}_I)$, $b_j(\mathbf{x}_I)$ are obtained by requiring the field function to pass through all the n field nodes in the local support domain, expressed in matrix form:

$$\mathbf{u}_s = \mathbf{R} \mathbf{a}(\mathbf{x}_I) + \mathbf{P} \mathbf{b}(\mathbf{x}_I) \quad (5)$$

where $\mathbf{u}_s = \{u_1, u_2, \dots, u_n\}^T$ is the vector of the field function parameters at the nodes of the local support domain, \mathbf{R} is the RBF moment matrix of size $n \times n$, and \mathbf{P} is the polynomial moment matrix of size $n \times m$. A unique solution to Equation (5) is obtained by applying the following constraint conditions [34]:

$$\sum_{i=1}^n p_j(\mathbf{x}_i) a_i(\mathbf{x}_I) = \mathbf{P}^T \mathbf{a}(\mathbf{x}_I) = 0, \quad j = 1, 2, \dots, m. \quad (6)$$

By combining Equations (5) and (6) the following equations are obtained:

$$\tilde{\mathbf{u}}_s = \begin{bmatrix} \mathbf{u}_s \\ \mathbf{0} \end{bmatrix} = \begin{bmatrix} \mathbf{R} & \mathbf{P} \\ \mathbf{P}^T & \mathbf{0} \end{bmatrix} \begin{bmatrix} \mathbf{a}(\mathbf{x}_I) \\ \mathbf{b}(\mathbf{x}_I) \end{bmatrix} = \mathbf{G}\mathbf{a}_0(\mathbf{x}_I) \quad (7)$$

and the unique solution is given by:

$$\mathbf{a}_0(\mathbf{x}_I) = \begin{Bmatrix} \mathbf{a}(\mathbf{x}_I) \\ \mathbf{b}(\mathbf{x}_I) \end{Bmatrix} = \mathbf{G}^{-1}\tilde{\mathbf{u}}_s. \quad (8)$$

To ensure that \mathbf{G}^{-1} is not singular, \mathbf{R}^{-1} should exist. The existence requirement is usually satisfied, even for arbitrarily scattered nodes [35, 36], rendering RPI a stable approximation method. Finally, the RPI basis functions:

$$\boldsymbol{\phi}(\mathbf{x}_I) = \{\phi_1(\mathbf{x}_I) \quad \phi_2(\mathbf{x}_I) \quad \dots \quad \phi_n(\mathbf{x}_I)\}^T \quad (9)$$

can be obtained by writing the approximation function as follows:

$$u^h(\mathbf{x}_I) = \{\mathbf{r}^T(\mathbf{x}_I) \quad \mathbf{p}^T(\mathbf{x}_I)\} \begin{Bmatrix} \mathbf{a}(\mathbf{x}_I) \\ \mathbf{b}(\mathbf{x}_I) \end{Bmatrix} = \{\mathbf{r}^T(\mathbf{x}_I) \quad \mathbf{p}^T(\mathbf{x}_I)\} \mathbf{G}^{-1}\tilde{\mathbf{u}}_s = \boldsymbol{\phi}^T(\mathbf{x}_I)\mathbf{u}_s = \sum_{i=1}^n \phi_i(\mathbf{x}_I)u_i. \quad (10)$$

The derivatives of $u^h(\mathbf{x})$ are easily obtained by:

$$u_{,J}^h(\mathbf{x}_I) = \phi_{,J}^T(\mathbf{x}_I)\mathbf{u}_s. \quad (11)$$

where J denotes spatial coordinate and the comma symbol designates a partial differentiation with respect to J .

3 Radial Point Interpolation Mixed Collocation Method

In this section the theoretical aspects of the Radial Point Interpolation Mixed Collocation (RPIMC) method and its computer implementation are described. The RPIMC theoretical formulation is based on the principles of the Meshless Local Petrov Galerkin Mixed Collocation (MLPG-MC), however the RPI basis function is used as trial function instead of the MLS. Without losing generality, from now on the field variable u represents the temperature field.

3.1 Theoretical aspects

Let's consider the balance equation of heat transfer in a domain Ω with boundary $\partial\Omega = \partial\Omega_u \cup \partial\Omega_q$ given by:

$$c\rho \frac{\partial u(\mathbf{x}, t)}{\partial t} + \nabla \cdot \mathbf{q}(\mathbf{x}, t) = f(\mathbf{x}, t) \quad \text{in } \Omega \quad (12)$$

$$u(\mathbf{x}, t) = \bar{u}(\mathbf{x}, t) \quad \text{at } \partial\Omega_u \quad (13)$$

$$-\mathbf{n} \cdot k \nabla u(\mathbf{x}, t) = \bar{q}(\mathbf{x}, t) \quad \text{at } \partial\Omega_q \quad (14)$$

where c is the specific heat capacity, ρ is the material density, $u(\mathbf{x}, t)$ is the temperature field, $\mathbf{q}(\mathbf{x}, t)$ is the heat flux, $f(\mathbf{x}, t)$ denotes the sum of any heat sources acting in the domain Ω , \bar{u} is the prescribed value of the temperature field on the Dirichlet boundary $\partial\Omega_u$, \bar{q} is the prescribed value of the heat flux on the Neumann boundary $\partial\Omega_q$, \mathbf{n} is the outward unit vector normal to $\partial\Omega_q$ and k is the thermal diffusivity coefficient.

The heat flux \mathbf{q} can be expressed by the heat flux - temperature gradient relation as:

$$\mathbf{q}(\mathbf{x}, t) = -k \nabla u(\mathbf{x}, t). \quad (15)$$

By using the RPI basis functions (section 2) to interpolate $u(\mathbf{x}, t)$ and each component $q_J(\mathbf{x}, t)$ of the heat flux vector $\mathbf{q}(\mathbf{x}, t)$ at a field node \mathbf{x}_I :

$$u(\mathbf{x}_I, t) = \sum_{i=1}^n \phi^i(\mathbf{x}_I) u^i(t) \quad (16)$$

$$q_J(\mathbf{x}_I, t) = \sum_{i=1}^n \phi^i(\mathbf{x}_I) q_J^i(t) \quad (17)$$

where n is the number of field nodes in the local support domain of \mathbf{x}_I .

Combining Equations (15) and (16), the heat flux at a field node \mathbf{x}_I and time t can be obtained by:

$$\mathbf{q}(\mathbf{x}_I, t) = -k \nabla u(\mathbf{x}_I, t) = -k \sum_{i=1}^n \nabla \phi^i(\mathbf{x}_I) u^i(t), \quad I = 1, 2, \dots, N \quad (18)$$

where N is the number of field nodes in the discretization of the domain Ω . In matrix form, the heat flux \mathbf{q} at all field nodes \mathbf{x}_I , $I = 1, 2, \dots, N$, and time t can be written as:

$$\mathbf{q} = \mathbf{K}_a \mathbf{u} \quad (19)$$

where \mathbf{q} is a vector containing heat fluxes at field nodes, \mathbf{K}_a is a sparse matrix containing the partial derivatives of the RPI basis functions at the nodes in the local support of each field node scaled by $(-k)$ and \mathbf{u} is a time-dependent vector containing temperature values at field nodes.

Equation (12) evaluated at \mathbf{x}_I and a given time t can be written as:

$$c\rho \sum_{i=1}^n \phi^i(\mathbf{x}_I) \frac{\partial u^i(t)}{\partial t} + \sum_{i=1}^n \nabla \phi^i(\mathbf{x}_I) \mathbf{q}^i(t) = f(\mathbf{x}_I, t), \quad I = 1, 2, \dots, N \quad (20)$$

or, equivalently,

$$c\rho \sum_{i=1}^n \phi^i(\mathbf{x}_I) \frac{\partial u^i(t)}{\partial t} - k \sum_{i=1}^n (\nabla \cdot \nabla \phi^i(\mathbf{x}_I)) u^i(t) = f(\mathbf{x}_I, t), \quad I = 1, 2, \dots, N. \quad (21)$$

Equations (20) and (21) can be written in the equivalent matrix forms as:

$$\mathbf{M} \dot{\mathbf{u}} + \mathbf{K}_s \mathbf{q} = \mathbf{f} \quad (22)$$

$$\mathbf{M} \dot{\mathbf{u}} + \mathbf{K} \mathbf{T} = \mathbf{f}, \quad \mathbf{K} = \mathbf{K}_s \mathbf{K}_a \quad (23)$$

where \mathbf{f} is an $N \times 1$ vector dependent on time t containing the values of $f(\mathbf{x}_I, t)$ for all field nodes \mathbf{x}_I , $I = 1, 2, \dots, N$.

3.2 Boundary conditions imposition

To impose Dirichlet BCs (Equation (13)), the collocation method is used. Prescribed temperature values at discrete points \mathbf{x}_I on the Dirichlet boundary $\partial\Omega_u$ are set by:

$$\sum_{i=1}^n \phi^i(\mathbf{x}_I) u^i(t) = \bar{u}(\mathbf{x}_I, t). \quad (24)$$

with n being the number of field nodes in the local support domain of \mathbf{x}_I . Due to the Kronecker delta property of the RPI basis functions, Dirichlet BCs are satisfied exactly in the RPIMC method. This is in contrast to the MLPG-MC, in which special treatment for the Dirichlet BCs is required due to the lack of the Kronecker delta property of the MLS basis functions.

To impose Neumann BCs (Equation (14)), the penalty method described in [37] is adopted. First, \mathbf{K}_s and \mathbf{K}_a matrices are splitted such that $\mathbf{K}_s^T = [\mathbf{K}_s^1 \ \mathbf{K}_s^2]$ and $\mathbf{K}_a^T = [\mathbf{K}_a^1 \ \mathbf{K}_a^2]$, where superscript 1 corresponds to the γ_r nodes in the $\partial\Omega_q$ boundary (Neumann nodes) and superscript 2 corresponds to the γ_u nodes in the $\partial\Omega_u$ boundary (Dirichlet nodes) and the interior of the domain Ω , such that the total number of nodes is $N = \gamma_r + \gamma_u$. For a given time t , Equation (14) is expressed in matrix form as:

$$\mathbf{N}_r \mathbf{q}^1 = \bar{\mathbf{q}}_r \quad (25)$$

where \mathbf{q}^1 is the vector of the nodal heat flux for the γ_r nodes. The matrix \mathbf{N}_r of the normal vectors and the vector $\bar{\mathbf{q}}_r$ of the prescribed heat flux values for the γ_r Neumann nodes are given by:

$$\mathbf{N}_r = \begin{bmatrix} \mathbf{n}^1 & & 0 \\ & \ddots & \\ 0 & & \mathbf{n}^{\gamma_r} \end{bmatrix} \quad \text{and} \quad \bar{\mathbf{q}}_r = \begin{bmatrix} \bar{q}^1 \\ \vdots \\ \bar{q}^{\gamma_r} \end{bmatrix}. \quad (26)$$

To enforce the Neumann BC, Equation (25) is multiplied by the penalty factor $\alpha \mathbf{N}_r^T$ and added to the components of Equation (19) corresponding to the Neumann nodes to obtain:

$$\mathbf{q}^1 + \alpha \mathbf{N}_r^T \mathbf{N}_r \mathbf{q}^1 = \mathbf{K}_a^1 \mathbf{u} + \alpha \mathbf{N}_r^T \bar{\mathbf{q}}_r. \quad (27)$$

By rearranging terms, Equation (27) can be written as:

$$\begin{aligned} \mathbf{q}^1 &= \{\mathbf{I} + \alpha \mathbf{N}_r^T \mathbf{N}_r\}^{-1} \{\mathbf{K}_a^1 \mathbf{u} + \alpha \mathbf{N}_r^T \bar{\mathbf{q}}_r\} \\ &= \mathbf{Q}^{-1} \{\mathbf{K}_a^1 \mathbf{u} + \alpha \mathbf{N}_r^T \bar{\mathbf{q}}_r\}, \end{aligned} \quad (28)$$

where \mathbf{I} is the identity matrix and $\mathbf{Q} = \mathbf{I} + \alpha \mathbf{N}_r^T \mathbf{N}_r$. Combining Equations (22) and (28), the matrix form of the modified heat transfer balance equation is given by:

$$\mathbf{M} \dot{\mathbf{u}} + \mathbf{K}' \mathbf{u} = \mathbf{f} - \alpha \mathbf{K}_s^1 \mathbf{Q}^{-1} \mathbf{N}_r^T \bar{\mathbf{q}}_r, \quad (29)$$

where $\mathbf{K}' = \mathbf{K}_s^1 \mathbf{Q}^{-1} \mathbf{K}_a^1 + \mathbf{K}_s^2 \mathbf{K}_a^2$.

3.3 Computer implementation

Regularly distributed nodes with equidistant spacing h in all coordinates are considered. The RPI shape parameters are selected as $\alpha_c = 1.5$, $d_c = h$ and $q = 1.03$. The penalty factor $\alpha = 10^6$ is chosen to enforce Neumann BCs through the penalty method. The standard forward finite difference scheme (forward Euler) with mass lumping is used to approximate partial differentiation with respect to time explicitly. The forward Euler method is well-known as a conditionally stable method. To ensure stability, an adequately small time step must be used. An estimation of the stable time step is computed by applying the Gerschgorin theorem [38]:

$$dt_s = \min_{i=1, \dots, n} \left[\frac{m_{ii}}{k_{ii} + \sum_{\substack{j=1 \\ j \neq i}}^n |k_{ij}|} \right]. \quad (30)$$

where m_{ii} , k_{ii} are the diagonal entries in \mathbf{M} and \mathbf{K}' matrices, respectively. The selected time step $dt = (0.9)dt_s$ is chosen after applying a 10% reduction to the stable time step to ensure the stability of the time integration. Finally, the pseudo-code of the RPIMC method's computer implementation is given in Algorithm (1).

Algorithm 1 Radial Point Interpolation Mixed Collocation (RPIMC) algorithm

```

1: procedure RPIMC( $\Omega, t_f$ )                                ▷ The RPIMC solution in domain  $\Omega$  for time  $[0, t_f]$ 
2:   initialize field variable:  $u = 0$ 
3:   distribute field nodes in domain  $\Omega$ 
4:   compute normals for boundary field nodes
5:   for <each field node  $i$ > do
6:     find field nodes in the local support domain of  $i$ 
7:     compute basis functions and derivatives
8:     assemble matrices:  $K_s^1, K_s^2, K_a^1, K_a^2, M$ 
9:     if  $i$  is on Neumann boundary  $\Gamma$  then
10:      assemble matrix:  $N_r$ 
11:    end if
12:  end for
13:  assemble matrices:  $Q, K'$ 
14:  compute  $dt$                                               ▷ Using Gerschgorin Theorem, Equation (30)
15:  while  $t \leq t_f$  do
16:    update body source:  $f$ 
17:    update field variable:  $u$                                 ▷ Using Forward Euler scheme
18:     $t = t + dt$ 
19:  end while
20: end procedure

```

4 Numerical Benchmarks

The performance of the RPIMC method is presented for several 2D and 3D heat transfer benchmark problems for which an analytical solution is available. Convergence analysis for the numerical solution u^h against the analytical solution u^{an} is performed in terms of the E_2 and $NRMS$ error metrics given by:

$$\begin{aligned}
 E_2 &= \left(\frac{\sum_{\mathbf{x}_i \in \Omega} (u^h(\mathbf{x}_i) - u^{an}(\mathbf{x}_i))^2}{\sum_{\mathbf{x}_i \in \Omega} u^{an}(\mathbf{x}_i)^2} \right)^{1/2}, \\
 NRMS &= \frac{\left(\sum_{\mathbf{x}_i \in \Omega} (u^h(\mathbf{x}_i) - u^{an}(\mathbf{x}_i))^2 \right)^{1/2}}{\max |u^{an}(\mathbf{x}_i)| - \min |u^{an}(\mathbf{x}_i)|}.
 \end{aligned} \tag{31}$$

For comparison, the benchmark problems are additionally solved with the MLPG-MC and FEM methods and convergence analysis is performed for these two methods. The convergence rate ($\bar{\rho}$) for the E_2 and $NRMS$ error metrics at successive refinements are calculated at the final simulation time $t = t_f$ using Equation (32), as proposed in [39]:

$$\bar{\rho} = \frac{\log\left(\frac{E_a}{E_b}\right)}{\log\left(\frac{h_a}{h_b}\right)} \tag{32}$$

where E_a, E_b denote the error and h_a, h_b the nodal spacing at two successive refinements. For the MLPG-MC method, the MLS basis function with linear polynomial basis is used as trial function and the quartic spline function as test function. FEM simulations are performed by using linear triangle and tetrahedral elements in 2D and 3D problems, respectively.

4.1 Lateral heat loss in 2D with Dirichlet boundary conditions

A heat conduction problem with lateral heat loss is solved in a 2D square domain Ω with edge length $l = 1$. The problem is described by the PDE:

$$u_{,0} = u_{,xx} + u_{,yy} + (1 + t^2)u + (2\pi^2 - t^2 - 2) \times \sin(\pi x)\cos(\pi y), \quad (x, y) \in \Omega, \quad t > 0 \tag{33}$$

with Dirichlet BCs on $\partial\Omega$:

$$\begin{aligned} u(0, y, t) &= u(1, y, t) = 0, \\ u(x, 0, t) &= u(x, 1, t) = e^{-t} \sin(\pi x), \end{aligned} \quad (34)$$

The initial condition can be obtained by the analytical solution for $t = 0$:

$$u(x, y, t) = e^{-t} \sin(\pi x) \cos(\pi y). \quad (35)$$

The problem is solved for the time interval $t = [0, 1]$ for 11×11 regularly distributed nodes in Ω with spatial spacing $h = 0.1$. Figure (1) shows the profiles of the solution for $y = 1$ and for $x = 0.5$, respectively. Convergence analysis is performed for successive refinements with $h = [0.1, 0.05, 0.025, 0.0125]$. The convergence analysis results for the E_2 and $NRMS$ error metrics are presented in Figure (2). A summary of the convergence rates for E_2 and $NRMS$ error metrics is provided in Table 1 and Table 2.

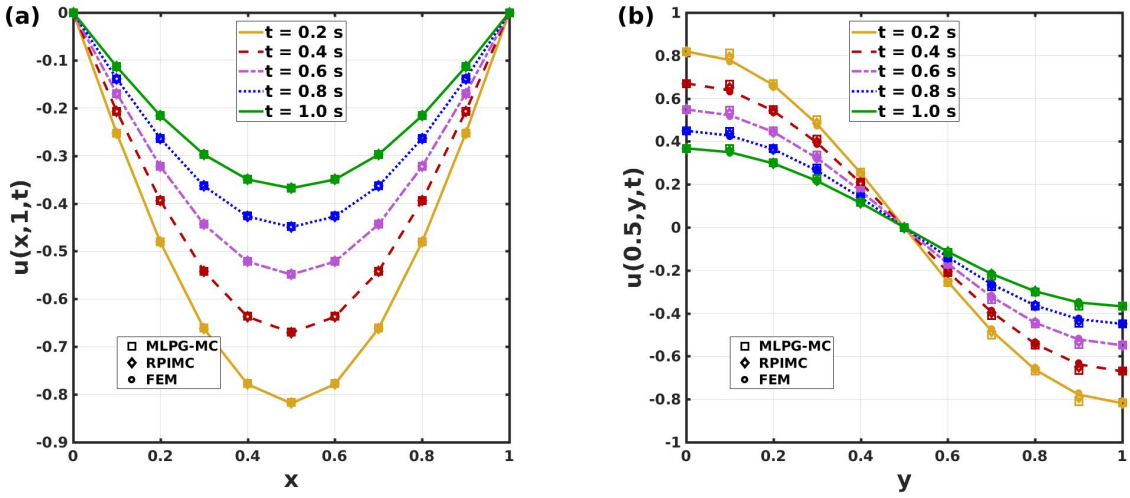


Figure 1: Solution for heat conduction with lateral heat loss in 2D for $t = [0, 1]$ using RPIMC (\diamond), MLPG-MC (\square), FEM (\circ). Plotted lines correspond to the analytical solution. (a) Solution profile for $y = 1$. (b) Solution profile for $x = 0.5$.

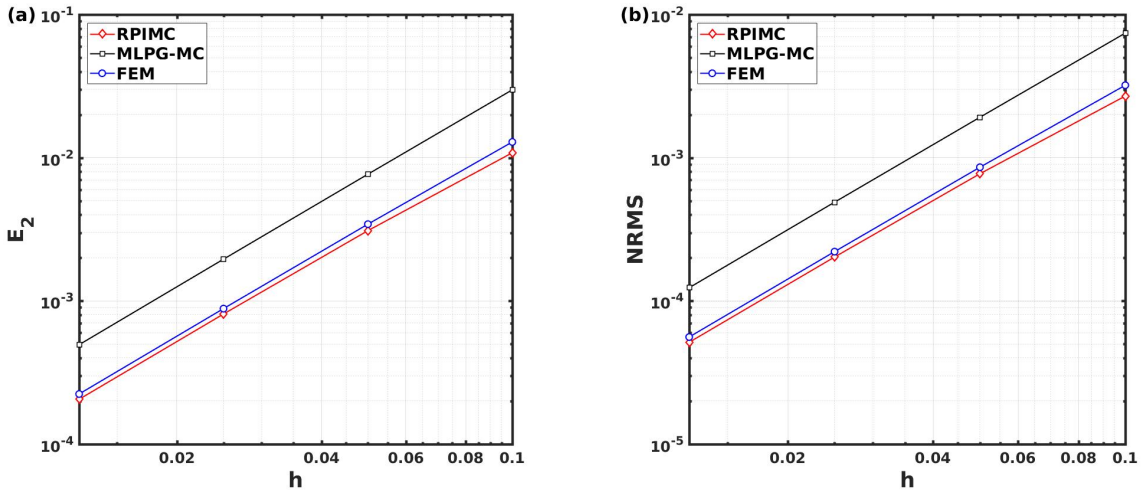


Figure 2: Convergence for heat conduction with lateral heat loss in 2D at $t = 1$ using RPIMC (\diamond), MLPG-MC (\square), FEM (\circ). (a) Convergence in E_2 error metric. (b) Convergence in $NRMS$ error metric.

4.2 Heat conduction in 3D with insulated borders

A heat conduction problem with insulated borders is solved in a 3D cubic domain Ω with edge length $l = \pi$. The problem is governed by the PDE:

$$u_{,0} = u_{,xx} + u_{,yy} + u_{,zz}; \quad (x, y, z) \in \Omega, \quad t > 0, \quad (36)$$

with Neumann BCs on $\partial\Omega$:

$$u_{,x}|_{x=0} = u_{,x}|_{x=\pi} = u_{,y}|_{y=0} = u_{,y}|_{y=\pi} = u_{,z}|_{z=0} = u_{,z}|_{z=\pi} = 0, \quad (37)$$

The initial condition is obtained by the analytical solution for $t = 0$:

$$u(x, y, z, t) = 1 + 2e^{-3t}\cos(x)\cos(y)\cos(z) + 3e^{-29t}\cos(2x)\cos(3y)\cos(4z). \quad (38)$$

The problem is solved for the time interval $t = [0, 1]$ for 11×11 regularly distributed nodes in Ω with spatial spacing $h = \pi/10$. Figure (3) shows the profiles of the solution for $y = z = \pi/5$ and $x = y = \pi/5$. Convergence analysis is performed for successive refinements with $h = [\pi/10, \pi/20, \pi/30, \pi/40]$. The convergence analysis results for the E_2 and $NRMS$ error metrics are presented in Figure(4). A summary of the convergence rates for E_2 and $NRMS$ error metrics is provided in Table 1 and Table 2.

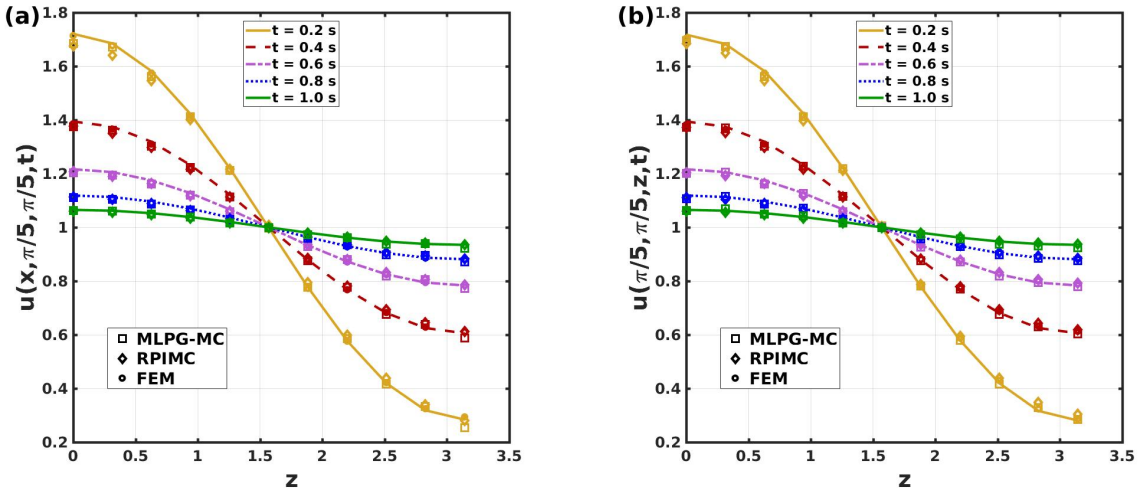


Figure 3: Solution for heat conduction with insulated borders in 3D for $t = [0, 1]$ using RPIMC (\diamond), MLPG-MC (\square), FEM (\circ). Plotted lines correspond to the analytical solution. (a) Solution profile for $y = z = \pi/5$. (b) Solution profile for $x = y = \pi/5$.

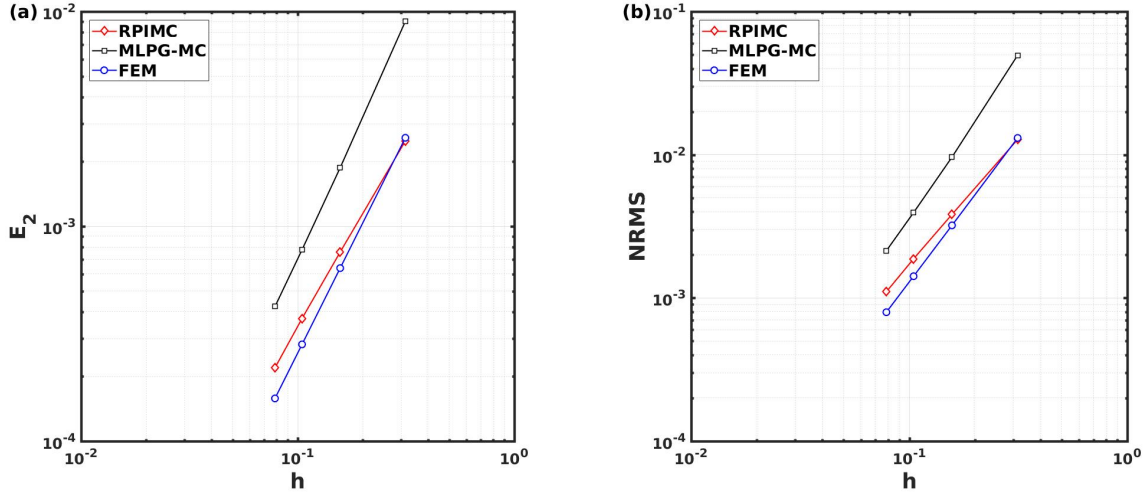


Figure 4: Convergence for heat conduction with insulated borders in 3D at $t = 1$ using RPIMC (\diamond), MLPG-MC (\square), FEM (\circ). (a) Convergence in E_2 error metric. (b) Convergence in $NRMS$ error metric.

4.3 Inhomogeneous heat conduction in 3D with Dirichlet boundary conditions

An inhomogeneous heat conduction problem with Dirichlet BCs is solved in a 3D cubic domain with edge length $l = \pi$. The problem is described by the following PDE:

$$u_{,0} = u_{,xx} + u_{,yy} + u_{,zz} + \sin(z); \quad 0 < x, y, z < \pi, \quad t > 0, \quad (39)$$

with the following Dirichlet BCs:

$$u(0, y, z, t) = \sin(z) + e^{-2t} \sin(y) \quad (40)$$

$$u(\pi, y, z, t) = \sin(z) - e^{-2t} \sin(y) \quad (41)$$

$$u(x, 0, z, t) = \sin(z) + e^{-2t} \sin(x) \quad (42)$$

$$u(x, \pi, z, t) = \sin(z) - e^{-2t} \sin(x) \quad (43)$$

$$u(x, y, 0, t) = u(x, y, \pi, t) = e^{-2t} \sin(x + y) \quad (44)$$

The initial condition is obtained by the analytical solution for $t = 0$:

$$u(x, y, z, 0) = \sin(z) + e^{-2t} \sin(x + y). \quad (45)$$

The problem is solved for the time interval $t = [0, 1]$ for 11×11 regularly distributed nodes in Ω with spatial spacing $h = \pi/10$. Figure (5) shows the profiles of the solution for $y = z = \pi/2$ and for $x = y = 3\pi/5$. Convergence analysis is performed for successive refinements with $h = [\pi/10, \pi/20, \pi/30, \pi/40]$. The convergence analysis results for the E_2 and $NRMS$ error metrics are presented in Figure(6). A summary of the convergence rates for E_2 and $NRMS$ error metrics is provided in Table 1 and Table 2.

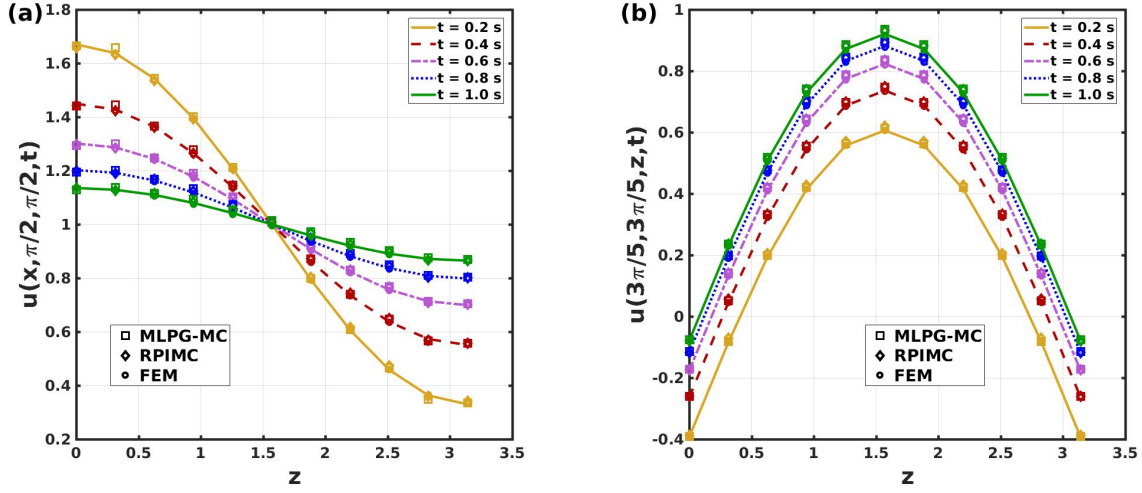


Figure 5: Solution for inhomogeneous heat conduction in 3D with Dirichlet boundary conditions for $t = [0, 1]$ RPIMC (\diamond), MLPG-MC (\square), FEM (\circ). Plotted lines correspond to the analytical solution. (a) Solution profile for $y = z = \pi/2$. (b) Solution profile for $x = y = 3\pi/5$.

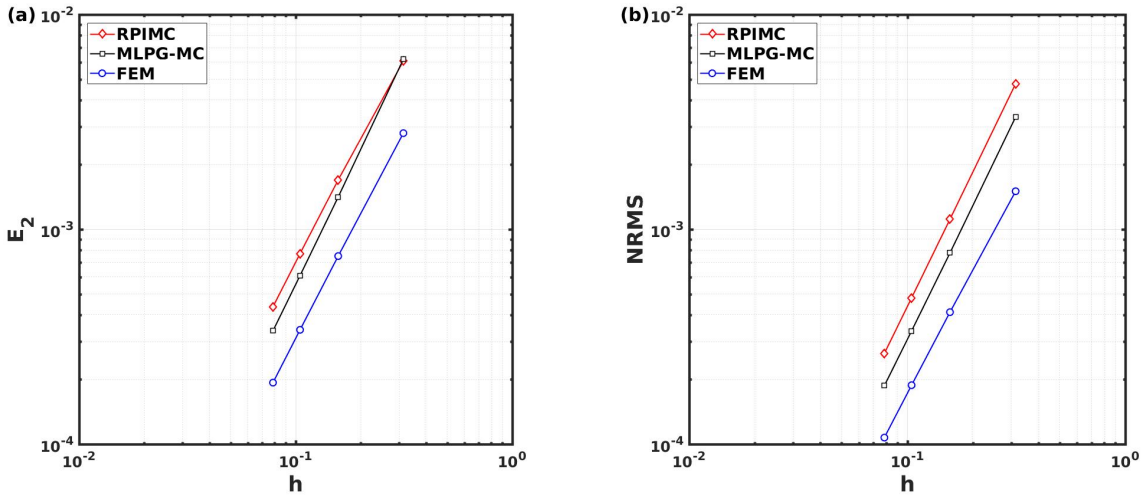


Figure 6: Convergence for inhomogeneous heat conduction with in 3D with Dirichlet boundary conditions at $t = 1$ using RPIMC (\diamond), MLPG-MC (\square), FEM (\circ). (a) Convergence in E_2 error metric. (b) Convergence in NRMS error metric.

Table 1: Summary of E_2 error metrics and convergence rates for all benchmarks.

h	E_2 error			Convergence rate ($\bar{\rho}$)		
	RPIMC	MLPG-MC	FEM	RPIMC	MLPG-MC	FEM
Benchmark 4.1: Lateral heat loss in 2D with Dirichlet boundary conditions						
0.1	1.08×10^{-2}	2.98×10^{-2}	1.29×10^{-2}	-	-	-
0.05	3.10×10^{-3}	7.70×10^{-3}	3.40×10^{-3}	1.81	1.96	1.91
0.025	8.00×10^{-4}	2.00×10^{-3}	9.00×10^{-4}	1.93	1.97	1.96
0.0125	2.00×10^{-4}	5.00×10^{-4}	2.00×10^{-4}	1.98	1.98	1.98
Benchmark 4.2: Heat conduction in 3D with insulated borders						
0.314	2.50×10^{-3}	9.00×10^{-3}	2.60×10^{-3}	-	-	-
0.157	8.00×10^{-4}	1.90×10^{-3}	6.00×10^{-4}	1.72	2.26	2.02
0.108	4.00×10^{-4}	8.00×10^{-4}	3.00×10^{-4}	1.76	2.17	2.02
0.079	2.00×10^{-4}	4.00×10^{-4}	2.00×10^{-4}	1.84	2.12	2.01
Benchmark 4.3: Inhomogeneous heat conduction in 3D with Dirichlet boundary conditions						
0.314	6.10×10^{-3}	6.20×10^{-3}	2.80×10^{-3}	-	-	-
0.157	1.70×10^{-4}	1.40×10^{-3}	8.00×10^{-4}	1.84	2.13	1.90
0.108	8.00×10^{-4}	6.00×10^{-4}	3.00×10^{-4}	1.95	2.08	1.95
0.079	4.00×10^{-4}	3.00×10^{-4}	2.00×10^{-4}	1.98	2.06	1.97

Table 2: Summary of NRMS error metrics and convergence rates for all benchmarks.

h	NRMS error			Convergence rate ($\bar{\rho}$)		
	RPIMC	MLPG-MC	FEM	RPIMC	MLPG-MC	FEM
Benchmark 4.1: Lateral heat loss in 2D with Dirichlet boundary conditions						
0.1	2.70×10^{-3}	7.42×10^{-3}	3.20×10^{-3}	-	-	-
0.05	7.73×10^{-4}	1.92×10^{-3}	8.58×10^{-4}	1.80	1.95	1.90
0.025	2.03×10^{-4}	4.89×10^{-4}	2.21×10^{-4}	1.93	1.97	1.96
0.0125	5.14×10^{-5}	1.24×10^{-4}	5.60×10^{-5}	1.98	1.98	1.98
Benchmark 4.2: Heat conduction in 3D with insulated borders						
0.314	1.28×10^{-2}	4.95×10^{-2}	1.31×10^{-2}	-	-	-
0.157	3.83×10^{-3}	9.63×10^{-3}	3.21×10^{-3}	1.74	2.36	2.03
0.108	1.88×10^{-3}	3.95×10^{-3}	1.42×10^{-3}	1.76	2.20	2.02
0.079	1.10×10^{-3}	2.14×10^{-3}	7.95×10^{-4}	1.84	2.13	2.01
Benchmark 4.3: Inhomogeneous heat conduction in 3D with Dirichlet boundary conditions						
0.314	4.77×10^{-3}	3.34×10^{-3}	1.50×10^{-3}	-	-	-
0.157	1.12×10^{-3}	7.77×10^{-4}	4.12×10^{-4}	2.10	2.10	1.87
0.108	4.80×10^{-4}	3.37×10^{-4}	1.88×10^{-4}	2.08	2.06	1.93
0.079	2.64×10^{-4}	1.87×10^{-4}	21.07×10^{-4}	2.07	2.04	1.95

5 Concluding remarks

The Meshless Local Petrov-Galerkin Mixed Collocation (MLPG-MC) method has been proven to be a time efficient and accurate numerical method for a large variety of problems. However, the use of the Moving Least Squares (MLS) as trial functions poses difficulties to the imposition of Dirichlet Boundary Conditions (BCs) due to the lack of the Kronecker delta property.

In the present study, the Radial Point Interpolation Mixed Collocation (RPIMC) method was implemented. RPIMC is a mixed collocation method where Radial Point Interpolation (RPI) basis functions are used as trial functions. RPI possess the delta Kronecker property and Dirichlet BCs are imposed similarly to FEM. The results achieved for a number of benchmark problems demonstrated that both the RPIMC and MLPG-MC methods can achieve high convergence rates in close proximity to the Finite Element Method (FEM) convergence rate. However, the RPIMC method has improved accuracy compared to the MLPG-MC, mainly due to the property of direct Dirichlet BC imposition.

In our simulations, the Forward Euler method was used to perform temporal integration. Being an explicit method, it is only conditionally stable and it would be more appropriate to use implicit integration or the Crank-Nicolson method, which are unconditionally stable. However, the motivation for this work is subsequent application of the developed method to the solution of action potential propagation in the human heart, which is described by a reaction-diffusion

PDE (monodomain model). In this context, the temporal integration time step is restricted by the reactive term, which is some orders of magnitude lower than the minimum stable time step for the diffusive term. Due to this restriction and the high parallelism of explicit time integration, the Forward Euler was considered as the method of choice. Nevertheless, the stability of the method was ensured by applying the Gercshg rin theorem for the estimation of a stable time step.

The RPIMC method is shown to be a promising alternative to FEM with similar convergence rate for the solution of transient diffusion problems, such as heat conduction. In future works, the RPIMC method will be applied to solve the monodomain model by using the operator splitting technique for the simulation of electrical propagation in the human heart. Importantly, the RPIMC method could additionally be extended to address other types of problems. In particular, it would an interest of ours to investigate its capabilities in addressing elastodynamics problems.

Acknowledgements

This work was supported by the European Research Council under the grant agreement ERC-2014-StG 638284, by MINECO (Spain) through project DPI2016-75458-R and by European Social Fund (EU) and Aragn Government through BSICoS group (T39.17R) and project LMP124-18. Computations were performed by the ICTS NANBIOSIS (HPC Unit at University of Zaragoza).

References

- [1] FP Incropera, AS Lavine, TL Bergman, and DP DeWitt. *Principles of heat and mass transfer*. Wiley-Blackwell, 2013.
- [2] S.V. Patankar and D.B. Spalding. A Calculation Procedure for Heat, Mass and Momentum Transfer in Three-dimensional Parabolic Flows. *Numerical Prediction of Flow, Heat Transfer, Turbulence and Combustion*, pages 54–73, jan 1983.
- [3] M. Hughes, K.A. Pericleous, and M. Cross. The CFD analysis of simple parabolic and elliptic MHD flows. *Applied Mathematical Modelling*, 18(3):150–155, mar 1994.
- [4] N. F. Britton. *Reaction-diffusion equations and their applications to biology*. Academic Press, 1986.
- [5] Gilbert Strang. On the Construction and Comparison of Difference Schemes. *SIAM Journal on Numerical Analysis*, 5(3):506–517, sep 1968.
- [6] Robert I. McLachlan and G. Reinout W. Quispel. Splitting methods. *Acta Numerica*, 11:341–434, jan 2002.
- [7] E.D. Skouras, G.C. Bourantas, V.C. Loukopoulos, and G.C. Nikiforidis. Truly meshless localized type techniques for the steady-state heat conduction problems for isotropic and functionally graded materials. *Engineering Analysis with Boundary Elements*, 35(3):452–464, mar 2011.
- [8] B.  sarler and R. Vertnik. Meshfree explicit local radial basis function collocation method for diffusion problems. *Computers & Mathematics with Applications*, 51(8):1269–1282, apr 2006.
- [9] Nicolas Libre, Arezoo Emdadi, Edward Kansa, Mohammad Rahimian, and Mohammad Shekarchi. A Stabilized RBF Collocation Scheme for Neumann Type Boundary Value Problems. *CMES - Computer Modeling in Engineering and Sciences*, 24(1):61–80, jan 2008.
- [10] T. Belytschko, Y. Y. Lu, and L. Gu. Element-free Galerkin methods. *International Journal for Numerical Methods in Engineering*, 37(2):229–256, jan 1994.
- [11] I. V. Singh, K. Sandeep, and Ravi Prakash. Heat Transfer Analysis of Two-dimensional Fins using Meshless Element Free Galerkin Method. *Numerical Heat Transfer, Part A: Applications*, 44(1):73–84, jul 2003.
- [12] I. V. Singh. Heat transfer analysis of composite slabs using meshless element Free Galerkin method. *Computational Mechanics*, 38(6):521–532, nov 2006.
- [13] Haitian Yang and Yiqian He. Solving heat transfer problems with phase change via smoothed effective heat capacity and element-free Galerkin methods. *International Communications in Heat and Mass Transfer*, 37(4):385–392, apr 2010.
- [14] Zan Zhang, JianFei Wang, YuMin Cheng, and Kim Meow Liew. The improved element-free Galerkin method for three-dimensional transient heat conduction problems. *Science China Physics, Mechanics and Astronomy*, 56(8):1568–1580, aug 2013.

- [15] Marino Arroyo and Michael Ortiz. Local maximum-entropy approximation schemes: a seamless bridge between finite elements and meshfree methods. *International journal for numerical methods in engineering*, 65(13):2167–2202, 2006.
- [16] Daniel Millán, N Sukumar, and Marino Arroyo. Cell-based maximum-entropy approximants. *Computer methods in applied mechanics and engineering*, 284:712–731, 2015.
- [17] Konstantinos A. Mountris, George C. Bourantas, Daniel Milln, Grand R. Joldes, Karol Miller, Esther Pueyo, and Adam Wittek. Cell-based maximum entropy approximants for three-dimensional domains: Application in large strain elastodynamics using the meshless total lagrangian explicit dynamics method. *International Journal for Numerical Methods in Engineering*, n/a(n/a).
- [18] Satya N. Atluri. *The meshless method (MLPG) for domain and BIE discretizations*. Tech Science Press, 2004.
- [19] S Li and SN Atluri. Topology-optimization of structures based on the MLPG mixed collocation method. *Computer Modeling in Engineering & Sciences*, 26(1):61, 2008.
- [20] ZD Han, AM Rajendran, and Satya N Atluri. Meshless local Petrov-Galerkin (MLPG) approaches for solving nonlinear problems with large deformations and rotations. *Computer Modeling in Engineering and Sciences*, 10(1):1, 2005.
- [21] Satya N. Atluri and Shengping Shen. The basis of meshless domain discretization: the meshless local Petrov-Galerkin (MLPG) method. *Advances in Computational Mathematics*, 23(1-2):73–93, jul 2005.
- [22] SN Atluri, ZD Han, AM Rajendran CMES: Computer Modeling In, and Undefined 2004. A new implementation of the meshless finite volume method, through the MLPG mixed approach. *Computer Modeling in Engineering & Sciences*, 6(6):491–514, 2004.
- [23] Satya N. Atluri, Hugh T. Liu, and Zdravko Dovedan Han. Meshless Local Petrov-Galerkin (MLPG) Mixed Collocation Method For Elasticity Problems. *Computer Modeling in Engineering & Sciences*, 4(3):141, 2006.
- [24] T Zhang, Y He, L Dong, S Li, A Alotaibi . . . Computer Modeling in . . . , and Undefined 2014. Meshless local petrov-galerkin mixed collocation method for solving cauchy inverse problems of steady-state heat transfer. *Computer Modeling in Engineering & Sciences*, 97(6):509–553, 2014.
- [25] G. R. Liu, G. Y. Zhang, Y. T. Gu, and Y. Y. Wang. A meshfree radial point interpolation method (RPIM) for three-dimensional solids. *Computational Mechanics*, 36(6):421–430, nov 2005.
- [26] G.R. Liu, G.Y. Zhang, Y.Y. Wang, Z.H. Zhong, G.Y. Li, and X. Han. A nodal integration technique for meshfree radial point interpolation method (NI-RPIM). *International Journal of Solids and Structures*, 44(11-12):3840–3860, jun 2007.
- [27] Y. L. Wu and G. R. Liu. A meshfree formulation of local radial point interpolation method (LRPIM) for incompressible flow simulation. *Computational Mechanics*, 30(5-6):355–365, apr 2003.
- [28] G.R. Liu and Y.T. Gu. A Local Radial Point Interpolation Method (LRPIM) for Free Vibration Analyses of 2-D Solids. *Journal of Sound and Vibration*, 246(1):29–46, sep 2001.
- [29] Y.T. Gu, Q.X. Wang, K.Y. Lam, and K.Y. Dai. A pseudo-elastic local meshless method for analysis of material nonlinear problems in solids. *Engineering Analysis with Boundary Elements*, 31(9):771–782, sep 2007.
- [30] Feng Wang, Gao Lin, Bao-Jing Zheng, and Zhi-Qiang Hu. An improved local radial point interpolation method for transient heat conduction analysis. *Chinese Physics B*, 22(6):060206, jun 2013.
- [31] G. R. Liu, Y. L. Wu, and H. Ding. Meshfree weak-strong (MWS) form method and its application to incompressible flow problems. *International Journal for Numerical Methods in Fluids*, 46(10):1025–1047, dec 2004.
- [32] M. Potse, B. Dube, J. Richer, A. Vinet, and R.M. Gulrajani. A Comparison of Monodomain and Bidomain Reaction-Diffusion Models for Action Potential Propagation in the Human Heart. *IEEE Transactions on Biomedical Engineering*, 53(12):2425–2435, dec 2006.
- [33] GR Liu. *Mesh free methods: moving beyond the finite element method*. CRC press, 2002.
- [34] M.A. Golberg, C.S. Chen, and H. Bowman. Some recent results and proposals for the use of radial basis functions in the BEM. *Engineering Analysis with Boundary Elements*, 23(4):285–296, apr 1999.
- [35] R.L. Hardy. Theory and applications of the multiquadric-biharmonic method 20 years of discovery 19681988. *Computers & Mathematics with Applications*, 19(8-9):163–208, jan 1990.
- [36] Holger Wendland. Error Estimates for Interpolation by Compactly Supported Radial Basis Functions of Minimal Degree. *Journal of Approximation Theory*, 93(2):258–272, may 1998.
- [37] Johannes TB Overvelde. The moving node approach in topology optimization. Master’s thesis, TU Delft, Delft University of Technology, 2012.

- [38] G. E. Myers. The Critical Time Step for Finite-Element Solutions to Two-Dimensional Heat-Conduction Transients. *Journal of Heat Transfer*, 100(1):120–127, feb 1978.
- [39] N. Thamareerat, A. Luadsong, and N. Ascharyaphotha. The meshless local PetrovGalerkin method based on moving Kriging interpolation for solving the time fractional NavierStokes equations. *SpringerPlus*, 5(1):417, dec 2016.